HHS Public Access

Author manuscript

Mol Psychiatry. Author manuscript; available in PMC 2023 September 01.

Published in final edited form as:

Mol Psychiatry. 2022 September ; 27(9): 3795–3805. doi:10.1038/s41380-022-01610-x.

Stress-Induced Changes of the Cholinergic Circuitry Promote Retrieval-Based Generalization of Aversive Memories

Lynn Y Ren[1], **Ana Cicvaric**[1,2], **Hui Zhang**[1,2], **Mariah AA Meyer**[1], **Anita L Guedea**[1], **Pan Gao**[1], **Zorica Petrovic**[2], **Xiaochen Sun**[4], **Yingxi Lin**[3,4], **Jelena Radulovic**[1,2,5,6]

[1]Department of Psychiatry and Behavioral Sciences, Northwestern University

[2]Dominick P. Purpura Department of Neuroscience, Albert Einstein College of Medicine

[3]Department of Psychiatry, State University of New York Upstate Medical University

[4]Department of Brain and Cognitive Sciences, Massachusetts Institute of Technology

[5]Department of Psychiatry and Behavioral Sciences, Albert Einstein College of Medicine

[6]Department of Biomedicine, Aarhus University

Abstract

Generalization, the process of applying knowledge acquired in one context to other contexts, often drives the expression of similar behaviors in related situations. At the cellular level, generalization is thought to depend on the activity of overlapping neurons that represent shared features between contexts (general representations). Using contextual fear conditioning in mice, we demonstrate that generalization can also occur in response to stress and result from reactivation of specific, rather than general context representations. We found that generalization emerges during memory retrieval, along with stress-induced abnormalities of septohippocampal oscillatory activity and acetylcholine release, which are typically found in negative affective states. In hippocampal neurons that represent aversive memories and drive generalization, cholinergic septohippocampal afferents contributed to a unique reactivation pattern of cFos, Npas4, and repressor element-1 silencing transcription factor (REST). Together, these findings suggest that generalization can be triggered by perceptually dissimilar but valence -congruent memories of specific aversive experiences. Through promoting the reactivation of such memories and their interference with

Correspondence: Jelena Radulovic, jelena.radulovic@einsteinmed.org, Jelena Radulovic, MD, PhD, Rose F. Kennedy Center, Room 115, 1410 Pelham Parkway South, Bronx, NY 10461, 718-430-2408.

CONTRIBUTIONS

LYR performed the behavioral, chemogenetic, and RAM experiments and data analysis and helped writing the manuscript. AC performed the optogenetic and fiber photometry experiments and analyzed the data, HZ performed the LFP experiments and data analyses, MAAM helped with the behavioral experiments and histochemical analyses, PG helped with the virus injection and expression analyses, ZP performed the circuit manipulations and RAM/REST studies, XS and YL provided all of the RAM constructs and shared key expertise in experimental design with RAM manipulations, JR designed the overall study, helped with data analysis, and wrote the manuscript.

Competing interests

The authors declare no competing financial interests.

Ethics declarations

Ethics approval

All animal procedures used in this study were approved by the Northwestern University IACUC and Albert Einstein Medical College IACUC and complied with federal regulations set forth by the National Institutes of Health.

ongoing behavior, abnormal cholinergic signaling could underlie maladaptive cognitive and behavioral generalization linked to negative affective states.

INTRODUCTION

Generalization allows information acquired in one situation to be applied to similar situations (1). However, inappropriate use of this cognitive strategy is maladaptive and is associated with psychiatric disorders such as major depressive disorder (MDD), generalized anxiety disorder (GAD), and posttraumatic stress disorder (PTSD) (2, 3). In MDD, overgeneralization is valence-independent and involves increased reporting of general memory features with concomitant loss of (or inability to access) specific memory details. In contrast, overgeneralization in PTSD seems to primarily involve increased accessibility of specific features of traumatic (i.e., negative) memories that interfere with ongoing cognitive functions (4). These differences show that delineating the neurobiology of different instances of generalization will inform our understanding of various psychopathologies and development of their treatments

Both in humans and animals, generalization has been mainly researched as a phenomenon that occurs during memory encoding and depends on perceptual similarities between (5) different experiences, which lead to increased overlap of shared (general) information (6). Generalization can also occur during memory retrieval, as recently demonstrated by a human study showing correlation between hippocampal activity at retrieval and behavioral generalization (7). Similarly, using aversive contextual conditioning in mice, we have shown that generalization can be induced after context memory consolidation through stress-induced modulation of memory retrieval (8). According to retrieval-based models of generalization, memory representations are “pattern separated” at encoding, and these representational overlaps are then inferred during retrieval (9). We do not know, however, how overlap is inferred at retrieval, especially if generalization occurs in a context sharing little or no similarity with the original representation.

At the neuronal level, there is increasing evidence that general and specific information are represented in different subsets of neurons, as revealed by studies using *in vivo* electrophysiology (10). This was confirmed with neuronal tagging and manipulation approaches using conditional, doxycycline (Dox)-regulated expression of robust activity marking (RAM) reporters in the dentate gyrus (DG). Using these approaches, it was shown that immediate early gene cFos- or Npas4-dependent RAM reporters, FRAM or NRAM reporters, respectively, contribute to the encoding of either general (FRAM) or specific (NRAM) context representations (11). Thus, manipulation of the reactivation patterns of these populations can be exploited to determine the contribution of general and specific memory representations to retrieval-based generalization.

Using context fear conditioning in mice, we recently found that social stress, when experienced after memory consolidation, can trigger retrieval-based generalization of an aversive contextual memory to an ambiguous context (8). Using this paradigm, we now demonstrate that stress-induced changes of cholinergic signaling, which include decreased low gamma power and altered acetylcholine (ACh) release, significantly promotes

generalization. This effect was mediated by cholinergic medial septal (MS) projections to dorsal hippocampus (DH) and DH muscarinic acetylcholine receptors (mAChRs). Stress-induced generalization (SIG) depended on the activation of NRAM, but not FRAM DG neurons, which displayed a unique, dual cFos/Npas4 co-reactivation pattern along with decreased levels of the repressor element-1 silencing transcription factor (REST). Inhibition of cholinergic septohippocampal projections partly normalized levels of REST+ and Npas4+ reactivation in N-RAM neurons, demonstrating a direct involvement of cholinergic signaling in NRAM reactivation contributing to generalization. These results suggest that by altering the cholinergic septohippocampal network, negative experiences can promote the reactivation of valence-congruent (negative) specific representations, which interferes with behavior by causing generalization. Given this, rectification of abnormal cholinergic signaling may be a promising therapeutic target for ameliorating overgeneralization phenotypes associated with stress.

METHODS

Mice (see Supplementary information)

We performed these experiments using male and female C57BL/6J mice and ChAT-Cre mice. Wild type C57BL/6J mice were purchased from Harlan (Indianapolis, IN). ChAt-Cre mice were obtained from the Jackson Laboratory (Bar Harbor, ME). The ChAT-Cre knockin mice, also known as ChAT-IRES-Cre, express Cre recombinase in cholinergic neurons (12). All mice were 8 weeks of age at the beginning of the experiments.

Contextual fear conditioning and generalization

Contextual fear conditioning was performed in an automated system (TSE Systems) (13). Mice were pre-exposed to Context A and Context B, each for 3 min. The contexts differed in shape (rectangular vs oval), flooring (grid vs smooth), light (75 vs 150 lux), and smell (alcohol vs acetic acid), and triggered similar exploratory behavior without inducing freezing in the absence of prior shock (Fig S1A). Exposures to these contexts were spaced 3 hours apart and counterbalanced except for the labeling experiments. After 24 hours, mice underwent 3 days of contextual fear conditioning. Each day consisted of a 3 min exposure to Context A, followed by a footshock (2 s, 0.7 mA, constant current). The next day, mice were tested for memory generalization by placing them into Context B for 3 min. Freezing was scored every 10 s during context exposures and expressed as a percentage of the total number of observations during which the mice were motionless. Mice were also tested for memory retrieval by returning them to the conditioning context (A) for 3 min. The Generalization Index was calculated as: 0.5 - (Context A - Context B)/(Context A + Context B). A higher generalization index indicates stronger generalization.

Social defeat stress and social instability stress

Social defeat stress was conducted by placing an “intruder” mouse (the experimental mouse) into the home cage of an aggressive “resident” mouse (CD-1 male mouse) for 5 min (8, 14). Experimental mice underwent social defeat once a day for 4 consecutive days.

Social instability stress was conducted by alternating cycles of 72 hours of housing with three other unfamiliar females and 24 hours of isolation while being single housed (8, 15, 16).

Stereotaxic surgeries and infusions of viral vectors and drugs (see Supplementary information)

Mice were anesthetized with isoflurane and 1.2% tribromoethanol (vol/vol, Avertin) for viral vector intracranial infusions and cannula implantations, respectively. The viral vectors carrying AAV8-hSyn-DIO-hM4D(Gi)-mCherry (Addgene 50475) or AAV5-Ef1a-DIO hChR2(E123T/T159C)-EYFP (Addgene 33509) were bilaterally infused into the MS (1mm anterior, 0 mm lateral, 4.5 mm ventral to bregma). The viral vector carrying AAV9-hSyn-GACh4.3 was purchased from WZ Biosciences, whereas AAV9-*F*-RAM-d2tTA-TRE-GFP, AAV9-*N*-RAM-d2tTA-TRE-GFP, AAV9-TRE-hM4Di-mCherry, AAV9-*F*-RAM-d2tTA-sEF1α-GFP, and AAV9-*N*-RAM-d2tTA-sEF1α-GFP were generated in the Yingxi Lin lab (MIT). The vectors were bilaterally infused into the DH or MS.

Bilateral 26-gauge guide cannulas (Plastics One) were placed in the DH, and CNO or scopolamine were infused through the cannulas 30 min prior to context retrieval or generalization. After the completion of behavioral testing, mice were intracardially perfused, and all brains were collected and cannula placements and virus spread were confirmed by immunohistochemical analysis of mCherry, EYFP, or GACh4.3 signals.

Implantation of devices for optogenetic stimulation (see Supplementary information)

All hardware and wireless devices for optogenetic stimulation were developed by and obtained from Neurolux (Urbana, IL) (17, 18). The implantation was performed 1 week before optogenetic stimulation and consisted of injecting the needle portion of the device into the brain and subdermal implantation of the body of the device on top of the skull. For optogenetic stimulation, mice were exposed to a wirelessly powered blue light photostimulation (473 nm, 3 min, tonic, 7 W) using 4 Hz or 20 Hz tonic stimulation or 20Hz bursts (1 sec on, 5 sec off). For within-group experiments, all mice were implanted with wireless optogenetic devices and light stimulation was on during either the first half or second half of the 180 second retrieval test, and this order was counterbalanced. For between-group experiments, mice were implanted with either a wireless optogenetic device or dummy device, and light stimulation was on during the entirety of the 180 second retrieval test.

LFP recordings and data analysis (see Supplementary information)

Two insulated silver electrodes were implanted into the MS and DH. A ground screw with a wire was lowered into the right interparietal bone and served as a reference and ground electrode. The LFP signals were recorded using a NeuroLogger (TSE Systems, Germany), a wireless 4-channel recording device in which pre-amplification, A-D conversion, and data storage are all included (19). All data were sampled at 500Hz.

Data analysis was performed by Matlab (MathWorks, USA), as previously described (20) (19, 21). Briefly, all data files were converted to a Matlab-compatible format. Spectral

analyses were performed using Chronux toolbox (http://Chronux.org). Coherence spectra were computed for the theta and gamma frequency bands using 35 half-overlapping 10 s windows with 4 tapers. Coherence was transformed using the Fisher z-transform and then normalized by power. Peak coherence in the theta and gamma bands were calculated for each mouse in each session and used for statistical analysis. Phase amplitude coupling was analyzed using the tPAC function of Brainstorm Matlab toolbox (22) with 1.1s slide time windows. After that the comodulograms were extracted for statistical analysis.

Fiberphotometry

To record fluorescent signals from pAAV-hSyn-GACh4.3-expressing neurons, we used 470 nm excitation LED. A 415 nm LED was used to acquire isosbestic control signal. The fluorescence signal was filtered and focused on a BlackFly CMOS camera and acquired at 40 FPS. The Neurophotometrics FP3001 system was used for data acquisition. Raw data were used as an input to Bonsai (23) and CropPolygon function was used to define ROIs. Synchronization with movement was provided by simultaneously triggering a TTL input from the fear conditioning system. A custom Matlab script was used to fit, scale, and subtract the isosbestic signal to correct for heat-induced LED decay and photobleaching. The signal was normalized to the background signal to obtain ΔF/F values. Change (%) in ΔF/F was used to average data across mice (24, 25). The fluctuation of Ach release in each mouse were determined by taking the sum of the squares of each ΔF/F deviation from the mean and dividing it by the number of values minus one. Maximal amplitude was determined by subtracting minimal from maximal ΔF/F value for each mouse.

Doxycycline (Dox)-regulated tagging experiments

Mice were placed on Doxycycline diet (625mg/kg, Envigo, Indianapolis, IN) ad libitum 1 day prior to viral infusion. The diet was discontinued 2 days before the Context A retrieval test to label activated FRAM or NRAM populations. The following day, the Dox diet was resumed until the end of the experiment.

Immunohistochemistry and immunofluorescence

One hour after re-exposure of mice to Context A (Context A -A reactivation or Context B (Context A-B reactivation), mice were intracardially perfused with ice-cold 4% paraformaldehyde in phosphate buffer (pH 7.4, 50 mL per mouse), brains were collected, and immunohistochemistry for GFP, Npas4, and cFos was performed on 50 μm free-floating sections (26) with primary antibodies against cFos (1:2,000, guinea pig, 226 308, Synaptic Systems), Npas4 (1:10,000, rabbit, Yingxi Lin (27)), or GFP (1:4000, chicken, Abcam ab13970). Brains of all mice were similarly collected and processed for analyzes of virus spread using anti-mCherry antibodies (1:1,000, rabbit, Abcam ab167453 or 1:16,000, chicken, ab205402). Secondary antibodies were obtained from Vector (1:300, biotinylated-anti chicken, anti-mouse, or anti-rabbit IgG). Sections were mounted using Vectashield (Vector) and observed with a confocal laser-scanning microscope (Olympus Fluoview FV10i) (8, 28). For light microscopy, signals were visualized with diaminobenzidine (Sigma) (28).

Image analysis and quantification

For cFos, GFP, and Npas4 co-localization analyses, flat images were obtained using a 10x objective on a Leica microscope with a Leica DFC450 C digital camera (28). All images were converted to binary format, and watershed segmentation was used to separate overlapping cells. Cell counts from hippocampal subregions were performed using two sections per mouse (1.8 mm posterior to bregma and 2.2 mm posterior to bregma) and averaged between two sections. Within hippocampal sections, a 200 μm^2 area of DG, a 200 μm^2 area of CA3, and a 100 μm^2 area of CA1 were defined. Only cells in a specific size range were counted, and a constant threshold was used to distinguish cells based on maximal signal to noise ratio. JACoP (Image J Plugin) object-based co-localization was used to determine co-localization by comparing the position of the centroids of the nuclei of the color channels. Their respective coordinates were then used to define structures separated by distances equal to or below the optical resolution. All quantifications were performed by an experimenter blind to treatment condition.

Quantification and statistical analyses

Statistical analyses were performed using GraphPad Prism. Data used for analyses included: (1) mice with virus expression in the MS or DH of 70% or more of the mean number of MS or DH-infected neurons across all experiments, (2) mice with detectable MS-originating terminals in the DH, and (3) mice with correctly implanted cannulas in the DH. For the behavioral studies, two-way RM ANOVA or three-way RM ANOVA with factors context, stress, and/or treatment, was used to determine group differences in freezing during Context A and Context B tests. Significant F values were followed by *post hoc* multiple comparisons using Tukey's or Sidak's tests. To calculate a generalization index, the same mice were exposed to both the conditioning Context A and Context B. Differences in the generalization index were also determined for treatment (CNO or Veh) or stress (Pre-Stress vs Post-Stress) using Mann-Whitney or Wilcoxon matched pairs signed rank text. Statistical differences were considered significant for all p values <0.05. In the graphs, significant effects of individual factors are indicated as straight lines whereas significant post-hoc differences between individual groups are indicated as connectors. All between subject analyses are presented as mean ± SEM with overlaid values for individual mice. Within subject analyses are presented as connected symbols for each individual mouse. Details of statistical analyses are found in figure legends.

Data and Code Availability

The data that support the findings of this study and the analysis code are available from the authors on reasonable request.

RESULTS

DH cholinergic signaling is altered by social defeat and contributes to stress-induced generalization

Memory retrieval depends on hippocampal oscillatory activity (29), which is controlled by inhibitory and cholinergic inputs from the MS. To determine whether social stress

triggers generalization (Fig S1B–D) by affecting oscillatory activity associated with memory retrieval, we recorded local field potentials (LFP) in the MS and DH of fear-conditioned mice during memory tests in Contexts A and B before and after social defeat (SD). Whereas theta and high gamma oscillations were not significantly affected by SD, the power of low gamma oscillations showed both context- and stress-dependent changes. Both before and after SD, the power of DH low gamma oscillations was significantly lower during retrieval tests in the conditioning Context A vs. the neutral Context B ($p<0.01$ and $p<0.001$, respectively). In response to SD, the power of DH low gamma oscillations during retrieval tests in both contexts was reduced in response to SD ($p<0.001$ for Context A and $p<0.05$ for Context B)(Fig 1A). Given the established role of cholinergic signaling in driving hippocampal low gamma oscillations (30, 31), we next monitored the ACh release dynamics before and after memory retrieval in non-stressed (NS) or SD mice using the ACh fluorescent sensor GACh4.3 (Fig 1B, Fig S2) (32). We found that SD, relative to NS, significantly affected the amplitude ($p<0.05$) and fluctuations ($p<0.05$) of fluorescent signals which were consistent with the slow (second to minute) muscarinic responses to ACh release in vivo (33) during memory retrieval (34, 35). Post-hoc analyses revealed a significant decrease in the amplitude of Ach signals during Context A retrieval ($p<0.05$), consistent with the greatest decrease of gamma power in this group. These findings suggested that, in parallel to SIG, SD alters the dynamics of DH oscillations and cholinergic signaling.

We next examined whether cholinergic modulation contributes to SIG, by infusing the mAChR antagonist scopolamine or vehicle (Veh) bilaterally into the DH of NS or SD mice before retrieval tests in Context A or B. SD mice, but not NS mice, injected with scopolamine froze significantly less in Context B vs. Context A ($p<0.001$), whereas SD mice injected with Veh did not (Fig 1C). Accordingly, the generalization index of scopolamine-infused SD mice was significantly reduced when compared to the Veh group ($p<0.01$)(Fig 1C). We replicated this finding with a different cohort of SD mice using a within-subject design. Consistent with our previous result, scopolamine significantly reduced freezing in Context B vs. Context A ($p<0.0001$). However, the next day on Veh, mice froze in Context B as strongly as in Context A, suggesting that the effects of scopolamine on SIG are transient (Fig S3). Lastly, scopolamine also reversed SIG in females (Fig S4A–C). Together, these findings suggest that SIG is a robust behavioral phenotype associated with SD-induced abnormalities of cholinergic signaling at the level of DH mAChRs.

Cholinergic septohippocampal projections contribute to stress-induced generalization

Similar to our findings in the DH, the power of low gamma oscillations in the MS also decreased as a function of context and stress (Fig 2A), however post-hoc comparisons did not reveal significant group differences. Unlike DH, the MS also showed corresponding changes in the power of high gamma oscillations. Surprisingly, although SD significantly affected local oscillations in both MS and DH, measures of connectivity between these brain areas known to affect memory recall, such as directional coherence (19) and theta-gamma phase amplitude coupling (36) (Fig S5), were not affected.

We next confirmed the presence of extensive DH cholinergic innervation stemming from the MS by injecting the anterograde tracer AAV-EF1a-DIO-eYFP into the MS of ChAt-Cre

mice (Fig 2B). To explore the role of these cholinergic septohippocampal projections in SIG, we infused AAV8-hSyn-DIO-hM4Gi-mCherry into the MS of mice subjected to fear conditioning and SD. Infusion of CNO in the DH of SD male mice expressing hM4Gi in cholinergic afferents from MS significantly reduced freezing in Context B ($p<0.001$), and the generalization index ($p<0.05$), without affecting freezing in Context A (Fig 2C). We previously ruled out nonspecific effects of DH-injected CNO on generalization (8). We performed the same experiment in female mice; however, our manipulations did not reduce SIG (Fig S4D–F), revealing a sex-specific neuromodulatory role of MS to DH cholinergic projections in SIG.

Optogenetic burst stimulation of cholinergic septohippocampal projections triggers SIG-like behavior

We next investigated whether stimulation of MS cholinergic terminals in the DH is sufficient to elicit generalization in male mice. We infused AAV2-EF1a-DIO-ChR2-eYFP into the MS and two weeks later, performed fear conditioning. The test was performed in NS mice in Context B while substituting SD with optogenetic stimulation. Tonic optogenetic stimulation with 4Hz or 20Hz during retrieval had no effect on freezing in Context B (Fig 3B,C, Fig S6A–C). On the other hand, 20Hz burst stimulation had a significant, enhancing effect on Context B freezing ($p<0.05$), (Fig 3D,E, Fig S6D). Consistent with this observation, in a replicate experiment using a between-subject design with either an optic fiber or dummy probe, we found that 20Hz burst stimulation eliminated the differences in freezing between Contexts A and B only in mice implanted with an optic fiber (Fig S6E). These results indicate that stimulation of MS cholinergic projections to the DH is sufficient to trigger generalization of freezing, as found in SIG.

Context A-activated NRAM neurons show SIG-specific reactivation patterns with Npas4 and cFos in the DG

Recent work has shown that different cellular ensembles in the DG encode the general and specific features of context memories and thus, promote contextual generalization and discrimination, respectively (11). These neuronal populations were identified using virally-encoded robust activity markers (RAM) driven by the immediate early genes cFos (FRAM, generalization) or Npas4 (NRAM, discrimination). We used this approach to further determine whether SIG is accompanied by changes of the reactivation patterns of these neuronal populations. Mice were kept on Dox diet starting one day before infusion of AAV9-*F*-RAM-d2tTA-TRE-GFP (FRAM-GFP) or AAV9-*N*-RAM-d2tTA-TRE-GFP (NRAM-GFP) into the DH. While on Dox diet, mice were fear conditioned in Context A and tested Context B. While off Dox, mice were tested in Context A to label FRAM or NRAM populations activated during the Context A retrieval test. The Dox diet was resumed until the end of the experiment when brains were collected from NS or SD mice 1 hour after the second retrieval test in Context A (Context A-A reactivation) or Context B (Context A-B reactivation) (Fig 4A, Fig 6A,B). Reactivation of the FRAM or NRAM neurons expressing GFP was determined by co-labelling with cFos and Npas4 (Fig S6–9). Control experiments with continuous Dox diet showed no fluorescent signals except for sparse CA1 neurons in FRAM-GFP-infused mice (Fig S6C–D).

Overall, in mice expressing FRAM, there were no significant stress condition or context differences in the number of GFP-, cFos-, or Npas4-positive DG neurons or the reactivation of the FRAM-GFP population ((Fig S7, Fig S8). Notably, all reactivated neurons were cFos-positive but Npas4-negative (Fig S7C, Fig S8B). Similarly, in NRAM-GFP expressing mice, the total number of GFP-, cFos-, or Npas4-positive DG neurons did not differ between groups (Fig 4). However, there were significant effects of reactivation context and SD on the reactivation patterns of NRAM-GFP. In both NS and SD mice, the number of Npas4/GFP-positive neurons were significantly higher in the Context A-B ($p<0.05$) when compared to the Context A-A condition. Moreover, whereas in the NS mice, Context A-B condition reactivation of the neurons were either cFos-positive (80%) or Npas4-positive (20%), in the same condition of SD mice, all Npas4-positive neurons were also cFos-positive (19%) ($p<0.01$ vs NS) (Fig 4C, S8B). This reactivation pattern was only found in the DG but not in the CA1 or CA3 DH subfields (Fig S9). Our findings thus reveal a subset of DG NRAM neurons activated during Context A retrieval that are reactivated during Context B retrieval, showing context- and stress-specific Npas4 signatures. The Npas4/cFos/GFP-positive reactivation pattern was uniquely seen during Contexts A-B retrieval that is accompanied by SIG.

We next investigated the functional relevance of FRAM and NRAM reactivation in SIG. FRAM or NRAM co-expressing the inhibitory designer receptor activated by designer drugs (AAV9-TRE-hM4Di-mCherry and either AAV9-*F*-RAM-d2tTA-sEF1α-GFP or AAV9-*N*-RAM-d2tTA-sEF1α-GFP) was infused into the DH to tag and inhibit the activity of FRAM or NRAM neuronal populations associated with memory retrieval in Context A (Fig 5A, C). Injection of CNO did not affect freezing in Contexts A or B or the generalization index in mice expressing FRAM Gi DREADD (Fig 5B). On the other hand, injection of CNO in mice expressing NRAM Gi DREADD significantly reduced freezing in Context B in the SD group without affecting freezing in Context A ($p<0.001$). Accordingly, SD mice receiving CNO had a significantly lower generalization index when compared to SD mice injected with Veh ($p<0.05$) (Fig 5D). These results showed that the NRAM population originally activated during Context A retrieval significantly contributes to SIG during Context B retrieval after SD. Thus, the specific Context A memory could gain predominant control over freezing behavior in Context B.

Septohippocampal cholinergic projections regulate NRAM reactivation after SD through REST/Npas4 signaling

In the last set of experiments, we investigated whether cholinergic septohippocampal inputs contribute to the reactivation of NRAM neurons after SD. Cholinergic signaling regulates gene expression by multiple mechanisms, some of which involve changes in REST (37, 38), which plays a major role in constraining Npas4 expression and activity. We found that after memory retrieval in Contexts A or B, nuclear REST levels in NRAM-GFP-positive neurons were significantly reduced in SD mice when compared to NS mice ($p<0.0001$) (Fig 6A–B). To determine whether cholinergic afferents from the MS contribute to the changes of REST levels in NRAM-labeled DG neurons, we injected AAV-DIO-hM4Gi DREADD in the MS and after 3 weeks, AAV9-*N*-RAM-d2tTA-TRE-GFP in the DH. After fear conditioning, context tests/labeling as previously described, and SD or NS, mice underwent

retrieval test in the presence of CNO or Veh. Injection of CNO into the DH of SD mice expressing Gi DREADD in cholinergic MS to DH projections significantly restored the nuclear levels of REST ($p<0.01$) and reduced the levels of Npas4 ($p<0.01$) (Fig 6C–E) in NRAM-GFP-positive DG neurons. These results suggest that SD-mediated Npas4/cFos/NRAM reactivation could be due to decreased nuclear REST at memory retrieval, resulting, at least in part, from cholinergic inputs from the MS.

DISCUSSION

Here, we demonstrate a retrieval-based mechanism of generalization of an aversive context memory, which is induced by stress and mediated by changes in cholinergic signaling in the septohippocampal network. Although SD consisted of only four sessions, it resulted in a robust generalization phenotype despite the many paradigm modifications required for the different experiments (labeling, pharmacological, and circuit manipulations). It also resulted in a decrease in the power of low gamma oscillations in the MS and DH, which is consistent with other literature consistently showing decreased gamma power in chronic stress models of depression in rodents (39, 40) and in depression in humans (41).

The generation of DH gamma power depends on ACh release, which showed significant abnormalities after social stress. Although our findings identified stress-induced alterations in ACh release, it remains to be established whether these abnormalities were associated with increased or decreased ACh levels. Several lines of evidence strongly support the former possibility. First, the power of hippocampal gamma oscillations is increased by low concentrations and decreased by high concentrations of the cholinergic agonist carbachol (30). Similarly, high ACh levels alter mAChR function, switching calcium oscillations from fluctuating to non-fluctuating patterns (42). Third, in our study, a hypercholinergic state is also suggested by the findings that optogenetic stimulation, but not inhibition, of cholinergic MS-DH projections induced generalization. This effective protocol with 20 Hz burst stimulation, is known to induce synaptic muscarinic responses in DH interneurons (43), induces reliable spiking in MS neurons (44), and corresponds to MS fast-firing patterns during behavioral activity *in vivo* (45). Lastly, the reduced REST levels in neurons reactivated after stress suggest cholinergic activation (46).

It is noteworthy that SIG in females did not involve the MS-DH circuit, consistent with the well-established sex-specific roles of cholinergic modulation in rodents (47) and humans (48), This was puzzling, however, given that, despite the usage of a different stress paradigm in females (8), DH cholinergic mechanisms played a significant role, as observed in males. Circuit mechanisms, such as stronger dependence of DH cholinergic signaling on diagonal band (of which was not targeted by our manipulations) rather than MS, could be one factor. Alternatively, intrinsic DH cholinergic mechanisms, which were recently found to contribute to aversively-motivated behavior (49), rather than circuit mechanisms, could play a stronger role in females.

At the neuronal level, social stress could have induced generalization by at least two different mechanisms: (1) by retroactively increasing the activity of general representations or (2) by increasing the activity of specific representations, thus causing interference at

retrieval. Our findings point to the latter possibility. Retroactively increasing the activity of general representations does not seem likely because the number of total and activated FRAM was not affected by stress, and because inhibition of FRAM was ineffective at reducing SIG. Despite our negative findings, a role of FRAM neurons cannot be ruled out in instances of generalization associated with general negative affect rather than (stressful) event-specific experiences.

Unlike FRAM, the NRAM neurons were found to play an important role in stress-induced generalization. Their co-activation with neurons responding to Context B were most likely induced by some level of perceived overlap at retrieval, leading to interference and generalization. Accordingly, generalization was fully reversed by chemogenetic inhibition of the NRAM population. Several observations related to the neuronal reactivation are notable. Similar to FRAM, the NRAM reactivation was also predominantly cFos mediated in the A-A condition. However, in the A-B condition, there was a unique Npas4 reactivation. And in mice that received SD, there was a cFos+Npas4+ co-reactivation pattern, which indicates stronger activation of individual NRAM neurons.

A consistent puzzle is that most of these effects (low gamma oscillations, ACh release, and REST levels) were retrieval- but not context-specific, whereas all pharmacological, optogenetic, and chemogenetic manipulations, and neuronal reactivation patterns, were specific to the A-B condition and generalization. The inability of chemogenetic manipulations to reduce freezing in the A-A condition could be explained by a ceiling effect of multiple fear conditioning trials on freezing behavior. This, however, cannot explain the distinct patterns of NRAM reactivation found only in the A-B condition (Npas4+NRAM+ in non-stressed and cFos+Npas4+NRAM+ in stressed mice), but not A-A condition. We propose that the observed reactivation pattern is related to two processes. The first one is based on the ambiguity of Context B which may lead to co-activation of Context A and B representations in Context B and Npas4+NRAM+ reactivation. Such effect would not be expected to occur in the A-A condition, which would render manipulations ineffective in Context A. This mechanism is consistent with evidence linking stimulus ambiguity to generalization in the absence of perceptual similarity (50). The second process involves further potentiation of NRAM activity (cFos+Npas4+NRAM+), resulting from enhanced Context A retrieval due to its affective congruence with the negative cholinergic state (51). The latter mechanism is in line with the view that abnormal cholinergic signaling generates negative affect and negative bias (52). Importantly, the transcription factors cFos, Npas4, and REST are also important regulators of neuronal gene expression associated with synaptic plasticity and memory (53–55). Their recurring co-activation could thus result in the update (56, 57) and state-dependent reinterpretation of initially non-aversive memories. While aligning ambiguous experiences to negative affective states could, in the short term, resolve a conflict caused by their affective incongruence (58), it could ultimately lead to enduring, maladaptive generalization phenotypes in seemingly unrelated situations, as is commonly observed in individuals who suffer from anxiety disorders (50, 59, 60). Our findings also suggest that cholinergic circuits and downstream signaling are potential therapeutic targets for stress-related overgeneralization.

Supplementary Material

Refer to Web version on PubMed Central for supplementary material.

ACKNOWLEDGEMENTS:

We thank Gail Mandel (Oregon Health & Science University) for providing the REST antibody, Ryan Drenan (Wake Forest School of Medicine) for providing advice with behavioral analyses of Chat-Cre mice, John A. Kessler (Northwestern University) for helping us finalize the immunohistochemistry studies in his lab, and Gordon Shepherd (Northwestern University) for discussions and feedback on the circuit approaches.

FUNDING

This work was funded by NIMH grants MH078064 and MH108837 and Lundbeck Foundation grant R310-2018-3611 to JR, F30MH122130 and T32MH067564 to LR, and NS115543 to YL.

REFERENCES

1. Banich MT, Dukes P, & Caccamise D Generalization of knowledge: Multidisciplinary perspectives: Psychology Press; 2010.
2. Ono M, Devilly GJ, Shum DH. A meta-analytic review of overgeneral memory: The role of trauma history, mood, and the presence of posttraumatic stress disorder. Psychol Trauma 2016;8(2):157–64. [PubMed: 25961867]
3. Barry TJ, Chiu CPY, Raes F, Ricarte J, Lau H. The Neurobiology of Reduced Autobiographical Memory Specificity. Trends Cogn Sci 2018;22(11):1038–49. [PubMed: 30292785]
4. King MJ, MacDougall AG, Ferris SM, Levine B, MacQueen GM, McKinnon MC. A review of factors that moderate autobiographical memory performance in patients with major depressive disorder. J Clin Exp Neuropsychol 2010;32(10):1122–44. [PubMed: 20544462]
5. Bennett M, Vervoort E, Boddez Y, Hermans D, Baeyens F. Perceptual and conceptual similarities facilitate the generalization of instructed fear. J Behav Ther Exp Psychiatry 2015;48:149–55. [PubMed: 25863485]
6. Shohamy D, Wagner AD. Integrating memories in the human brain: hippocampal-midbrain encoding of overlapping events. Neuron 2008;60(2):378–89. [PubMed: 18957228]
7. Berens SC, Bird CM. The role of the hippocampus in generalizing configural relationships. Hippocampus 2017;27(3):223–8. [PubMed: 27933668]
8. Ren LY, Meyer MAA, Grayson VS, Gao P, Guedea AL, Radulovic J. Stress-induced generalization of negative memories is mediated by an extended hippocampal circuit. Neuropsychopharmacology 2021.
9. Kumaran D, McClelland JL. Generalization through the recurrent interaction of episodic memories: a model of the hippocampal system. Psychol Rev 2012;119(3):573–616. [PubMed: 22775499]
10. Yu JY, Liu DF, Loback A, Grossrubatscher I, Frank LM. Specific hippocampal representations are linked to generalized cortical representations in memory. Nat Commun 2018;9(1):2209. [PubMed: 29880860]
11. Sun X, Bernstein MJ, Meng M, Rao S, Sorensen AT, Yao L, et al. Functionally Distinct Neuronal Ensembles within the Memory Engram. Cell 2020;181(2):410–23 e17. [PubMed: 32187527]
12. Rossi J, Balthasar N, Olson D, Scott M, Berglund E, Lee CE, et al. Melanocortin-4 receptors expressed by cholinergic neurons regulate energy balance and glucose homeostasis. Cell Metab 2011;13(2):195–204. [PubMed: 21284986]
13. Corcoran KA, Donnan MD, Tronson NC, Guzman YF, Gao C, Jovasevic V, et al. NMDA receptors in retrosplenial cortex are necessary for retrieval of recent and remote context fear memory. J Neurosci 2011;31(32):11655–9. [PubMed: 21832195]
14. Golden SA, Covington HE, Berton O 3rd, Russo SJ A standardized protocol for repeated social defeat stress in mice. Nat Protoc 2011;6(8):1183–91. [PubMed: 21799487]

15. Goni-Balentziaga O, Perez-Tejada J, Renteria-Dominguez A, Lebena A, Labaka A. Social instability in female rodents as a model of stress related disorders: A systematic review. Physiol Behav 2018;196:190–9. [PubMed: 30196085]
16. Labaka A, Gomez-Lazaro E, Vegas O, Perez-Tejada J, Arregi A, Garmendia L. Reduced hippocampal IL-10 expression, altered monoaminergic activity and anxiety and depressive-like behavior in female mice subjected to chronic social instability stress. Behav Brain Res 2017;335:8–18. [PubMed: 28789949]
17. Shin G, Gomez AM, Al-Hasani R, Jeong YR, Kim J, Xie Z, et al. Flexible Near-Field Wireless Optoelectronics as Subdermal Implants for Broad Applications in Optogenetics. Neuron 2017;93(3):509–21 e3. [PubMed: 28132830]
18. Jeong JW, McCall JG, Shin G, Zhang Y, Al-Hasani R, Kim M, et al. Wireless Optofluidic Systems for Programmable In Vivo Pharmacology and Optogenetics. Cell 2015;162(3):662–74. [PubMed: 26189679]
19. Corcoran KA, Frick BJ, Radulovic J, Kay LM. Analysis of coherent activity between retrosplenial cortex, hippocampus, thalamus, and anterior cingulate cortex during retrieval of recent and remote context fear memory. Neurobiol Learn Mem 2016;127:93–101. [PubMed: 26691782]
20. Kay LM, Freeman WJ. Bidirectional processing in the olfactory-limbic axis during olfactory behavior. Behav Neurosci 1998;112(3):541–53. [PubMed: 9676972]
21. Rojas-Libano D, Frederick DE, Egana JI, Kay LM. The olfactory bulb theta rhythm follows all frequencies of diaphragmatic respiration in the freely behaving rat. Front Behav Neurosci 2014;8:214. [PubMed: 24966821]
22. Tadel F, Baillet S, Mosher JC, Pantazis D, Leahy RM. Brainstorm: a user-friendly application for MEG/EEG analysis. Comput Intell Neurosci 2011;2011:879716. [PubMed: 21584256]
23. Lopes G, Bonacchi N, Frazao J, Neto JP, Atallah BV, Soares S, et al. Bonsai: an event-based framework for processing and controlling data streams. Front Neuroinform 2015;9:7. [PubMed: 25904861]
24. Proulx CD, Aronson S, Milivojevic D, Molina C, Loi A, Monk B, et al. A neural pathway controlling motivation to exert effort. Proc Natl Acad Sci U S A 2018;115(22):5792–7. [PubMed: 29752382]
25. Martianova E, Aronson S, Proulx CD. Multi-Fiber Photometry to Record Neural Activity in Freely-Moving Animals. J Vis Exp 2019(152).
26. Jovasevic V, Corcoran KA, Leaderbrand K, Yamawaki N, Guedea AL, Chen HJ, et al. GABAergic mechanisms regulated by miR-33 encode state-dependent fear. Nat Neurosci 2015;18(9):1265–71. [PubMed: 26280760]
27. Lin Y, Bloodgood BL, Hauser JL, Lapan AD, Koon AC, Kim TK, et al. Activity-dependent regulation of inhibitory synapse development by Npas4. Nature 2008;455(7217):1198–204. [PubMed: 18815592]
28. Meyer MAA, Anstotz M, Ren LY, Fiske MP, Guedea AL, Grayson VS, et al. Stress-related memories disrupt sociability and associated patterning of hippocampal activity: a role of hilar oxytocin receptor-positive interneurons. Transl Psychiatry 2020;10(1):428. [PubMed: 33311459]
29. Duzel E, Penny WD, Burgess N. Brain oscillations and memory. Curr Opin Neurobiol 2010;20(2):143–9. [PubMed: 20181475]
30. Betterton RT, Broad LM, Tsaneva-Atanasova K, Mellor JR. Acetylcholine modulates gamma frequency oscillations in the hippocampus by activation of muscarinic M1 receptors. Eur J Neurosci 2017;45(12):1570–85. [PubMed: 28406538]
31. Fisahn A, Pike FG, Buhl EH, Paulsen O. Cholinergic induction of network oscillations at 40 Hz in the hippocampus in vitro. Nature 1998;394(6689):186–9. [PubMed: 9671302]
32. Jing M, Zhang P, Wang G, Feng J, Mesik L, Zeng J, et al. A genetically encoded fluorescent acetylcholine indicator for in vitro and in vivo studies. Nat Biotechnol 2018;36(8):726–37. [PubMed: 29985477]
33. Fadel JR. Regulation of cortical acetylcholine release: insights from in vivo microdialysis studies. Behav Brain Res 2011;221(2):527–36. [PubMed: 20170686]

34. Nail-Boucherie K, Dourmap N, Jaffard R, Costentin J. Contextual fear conditioning is associated with an increase of acetylcholine release in the hippocampus of rat. Brain Res Cogn Brain Res 2000;9(2):193–7. [PubMed: 10729702]
35. Zhang H, Lin SC, Nicolelis MA. Spatiotemporal coupling between hippocampal acetylcholine release and theta oscillations in vivo. J Neurosci 2010;30(40):13431–40. [PubMed: 20926669]
36. Radiske A, Gonzalez MC, Conde-Ocazionez S, Rossato JI, Kohler CA, Cammarota M. Cross-Frequency Phase-Amplitude Coupling between Hippocampal Theta and Gamma Oscillations during Recall Destabilizes Memory and Renders It Susceptible to Reconsolidation Disruption. J Neurosci 2020;40(33):6398–408. [PubMed: 32661022]
37. Hersh LB, Shimojo M. Regulation of cholinergic gene expression by the neuron restrictive silencer factor/repressor element-1 silencing transcription factor. Life Sci 2003;72(18–19):2021–8. [PubMed: 12628452]
38. Srivas S, Thakur MK. Transcriptional co-repressor SIN3A silencing rescues decline in memory consolidation during scopolamine-induced amnesia. J Neurochem 2018;145(3):204–16. [PubMed: 29494759]
39. Sauer JF, Struber M, Bartos M. Impaired fast-spiking interneuron function in a genetic mouse model of depression. Elife 2015;4.
40. Voget M, Rummel J, Avchalumov Y, Sohr R, Haumesser JK, Rea E, et al. Altered local field potential activity and serotonergic neurotransmission are further characteristics of the Flinders sensitive line rat model of depression. Behav Brain Res 2015;291:299–305. [PubMed: 26025511]
41. Fitzgerald PJ, Watson BO. Gamma oscillations as a biomarker for major depression: an emerging topic. Transl Psychiatry 2018;8(1):177. [PubMed: 30181587]
42. Rathouz MM, Vijayaraghavan S, Berg DK. Acetylcholine differentially affects intracellular calcium via nicotinic and muscarinic receptors on the same population of neurons. J Biol Chem 1995;270(24):14366–75. [PubMed: 7782297]
43. Bell LA, Bell KA, McQuiston AR. Activation of muscarinic receptors by ACh release in hippocampal CA1 depolarizes VIP but has varying effects on parvalbumin-expressing basket cells. J Physiol 2015;593(1):197–215. [PubMed: 25556796]
44. Ma X, Zhang Y, Wang L, Li N, Barkai E, Zhang X, et al. The Firing of Theta State-Related Septal Cholinergic Neurons Disrupt Hippocampal Ripple Oscillations via Muscarinic Receptors. J Neurosci 2020;40(18):3591–603. [PubMed: 32265261]
45. Brazhnik ES, Fox SE. Action potentials and relations to the theta rhythm of medial septal neurons in vivo. Exp Brain Res 1999;127(3):244–58. [PubMed: 10452212]
46. Salani M, Anelli T, Tocco GA, Lucarini E, Mozzetta C, Poiana G, et al. Acetylcholine-induced neuronal differentiation: muscarinic receptor activation regulates EGR-1 and REST expression in neuroblastoma cells. J Neurochem 2009;108(3):821–34. [PubMed: 19187099]
47. Mitsushima D Sex differences in the septo-hippocampal cholinergic system in rats: behavioral consequences. Curr Top Behav Neurosci 2011;8:57–71. [PubMed: 21769723]
48. Giacobini E, Pepeu G. Sex and Gender Differences in the Brain Cholinergic System and in the Response to Therapy of Alzheimer Disease with Cholinesterase Inhibitors. Curr Alzheimer Res 2018;15(11):1077–84. [PubMed: 29895246]
49. Mineur YS, Mose TN, Vanopdenbosch L, Etherington IM, Ogbejesi C, Islam A, et al. Hippocampal acetylcholine modulates stress-related behaviors independent of specific cholinergic inputs. Mol Psychiatry 2022.
50. Dunsmoor JE, Paz R. Fear Generalization and Anxiety: Behavioral and Neural Mechanisms. Biol Psychiatry 2015;78(5):336–43. [PubMed: 25981173]
51. Tulving E Cue-Dependent Forgetting. American Scientist 62(1):74–82.
52. Mineur YS, Picciotto MR. The role of acetylcholine in negative encoding bias: Too much of a good thing? Eur J Neurosci 2021;53(1):114–25. [PubMed: 31821620]
53. Weng FJ, Garcia RI, Lutzu S, Alvina K, Zhang Y, Dushko M, et al. Npas4 Is a Critical Regulator of Learning-Induced Plasticity at Mossy Fiber-CA3 Synapses during Contextual Memory Formation. Neuron 2018;97(5):1137–52 e5. [PubMed: 29429933]
54. Sun X, Lin Y. Npas4: Linking Neuronal Activity to Memory. Trends Neurosci 2016;39(4):264–75. [PubMed: 26987258]

55. Ramamoorthi K, Fropf R, Belfort GM, Fitzmaurice HL, McKinney RM, Neve RL, et al. Npas4 regulates a transcriptional program in CA3 required for contextual memory formation. Science 2011;334(6063):1669–75. [PubMed: 22194569]

56. Alberini CM, Milekic MH, Tronel S. Mechanisms of memory stabilization and destabilization. Cell Mol Life Sci 2006;63(9):999–1008. [PubMed: 16596332]

57. Stein M, Rohde KB, Henke K. Focus on emotion as a catalyst of memory updating during reconsolidation. Behav Brain Sci 2015;38:e27. [PubMed: 26050691]

58. Besnard A, Sahay A. Adult Hippocampal Neurogenesis, Fear Generalization, and Stress. Neuropsychopharmacology 2016;41(1):24–44. [PubMed: 26068726]

59. Lissek S, Kaczkurkin AN, Rabin S, Geraci M, Pine DS, Grillon C. Generalized anxiety disorder is associated with overgeneralization of classically conditioned fear. Biol Psychiatry 2014;75(11):909–15. [PubMed: 24001473]

60. Lissek S Toward an account of clinical anxiety predicated on basic, neurally mapped mechanisms of Pavlovian fear-learning: the case for conditioned overgeneralization. Depress Anxiety 2012;29(4):257–63. [PubMed: 22447565]

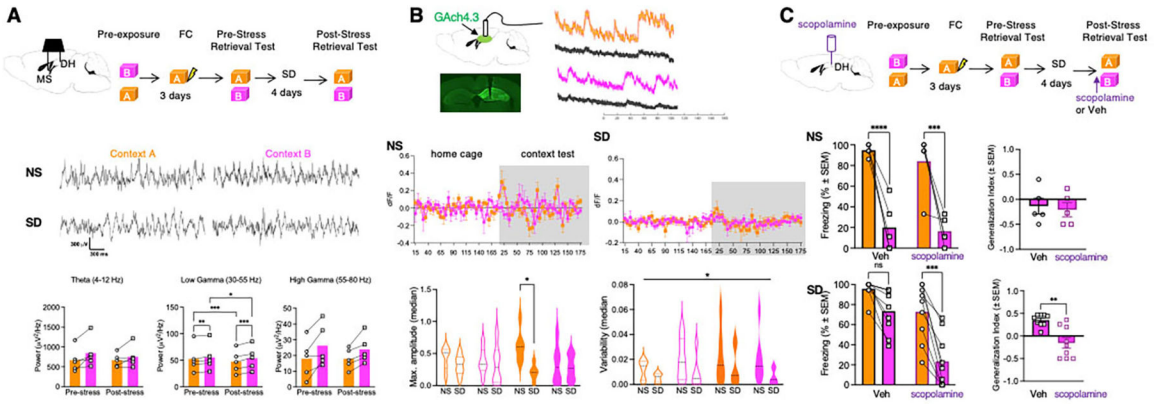

Fig 1: SD triggers abnormalities of hippocampal cholinergic signaling contributing to SIG

A Top, experimental design of LFP recordings performed during pre- and post-stress retrieval tests. Middle, traces of LFP recordings in Contexts A and B before and after SD. Bottom, stress- and context-dependent changes of DH oscillatory activity, n = 5 mice. Bottom Left: Two-way RM ANOVA. Factor: Stress, F (1, 4) = 0.6211, p=0.4747. Factor: Context, F (1, 4) = 4.589, p=0.0988. Factor: Stress x Context, F (1, 4) = 1.159, p=0.3424. Bottom Center: Two-way RM ANOVA. Factor: Stress, F (1, 4) = 0.7193, p=0.4442. Factor: Context, F (1, 4) = 53.55, p=0.0019. Factor: Stress x Context, F (1, 4) = F (1, 4) = 47.50, p=0.0023. Bottom Right: Two-way RM ANOVA. Factor: Stress, F (1, 4) = 0.1706, p=0.7008. Factor: Context, F (1, 4) = 19.37, p=0.0117. Factor: Stress x Context, F (1, 4) = 0.5711, p=0.4919. **B** Top, experimental design of fiber photometry of ACh release in NS and SD groups in the home cage after exposure to Contexts A and B. Middle, dynamics of ACh release during context exposure in NS and SD mice. In NS mice, two-way RM ANOVA revealed a significant Time x Context interaction indicative of fluctuations of Ach levels during context tests {Factor: Time, F (7.226, 115.6) = 1.636, p=0.1297. Factor: Context, F (3, 16) = 0.3821, p=0.7673. Factor: Time x Context, F (96, 512) = 1.621, p=0.0005. n=5 mice per group]. Such fluctuations of ACh release were disrupted during context exposure in SD mice [Two-way RM ANOVA. Factor: Time, F (5.374, 53.74) = 1.156, p=0.3434. Factor: Context, F (1, 10) = 0.1402, p=0.7159. Factor: Time x Context, F 65, 650) = 0.7276, p=0.9456. n=6 mice per group]. Bottom, left, significant decrease of maximal amplitude during Context A tests of SD relative to NS mice [F(1,40)= 6.127, p<0.0176]. Reduction of Ach fluctuations in SD mice was also found [F(1,40)= 6.332, p<0.016], however, there were no significant post-hoc differences. **C** Top, experimental design of hippocampal muscarinic receptor inhibition with scopolamine. Cannulation was performed 72 hours before behavioral tests. Middle, lack of scopolamine effects on freezing behavior in NS mice. Middle left: Two-way RM ANOVA. Factor: Drug, F (1, 8) = 0.7626, p=0.4080. Factor: Context, F (1, 8) = 52.64, p<0.0001. Factor: Drug x Context, F (1, 8) = 0.1269, p=0.7309, n = 5 mice per group. Middle right: Mann Whitney Test. p=0.8810. Sum of Ranks, 28.5, 26.5 (Veh, Scop). Bottom, reduced generalization of freezing in SD mice injected with scopolamine. Bottom left: Two-way RM ANOVA. Factor: Drug, F (1, 16) = 14.86, p=0.0014. Factor: Context, F (1, 16) = 52.74, p<0.0001. Factor: Drug x Context, F (1, 16) = 7.576, p=0.0142. n = 9 mice per group. Bottom right: Mann Whitney Test. p=0.0014. Sum of Ranks, 119.5, 51.5 (Veh, Scop).

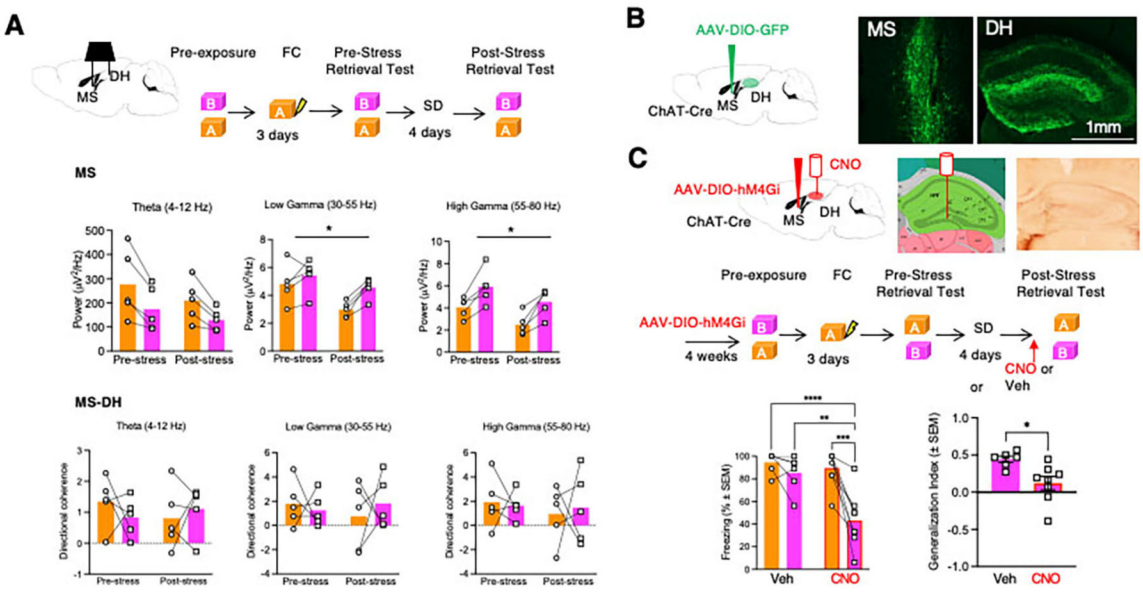

Fig 2: SD triggers changes in MS oscillations and induces SIG through MS-DH projections

A Top, experimental design of LFP recordings performed during the pre- and post-stress retrieval tests. Middle, stress- and context-dependent changes of MS oscillatory activity. n=5 mice in each group. Middle Left: Two-Way RM ANOVA. Factor: Stress, F (1, 4) = 2.824, p=0.1682. Factor: Context, F (1, 4) = 19.65. p=0.0114. Factor: Context x Stress, F (1, 4) = 1.586. p=0.2764. Middle Center: Two-Way RM ANOVA. Factor: Stress, F (1, 4) = 13.93, p=0.0203. Factor: Context, F (1, 4) = 13.76. p=0.0207. Factor: Context x Stress, F (1, 4) = 4.104. p=0.1127. Middle Right: Two-Way RM ANOVA. Factor: Stress, F (1, 4) = 32.04, p=0.0048. Factor: Context, F (1, 4) = 62.88. p=0.0014. Factor: Context x Stress, F (1, 4) = 0.07422. p=0.7988, n=5 mice per group. Bottom, lack of changes in the directional coherence of MS and DH oscillatory activity. Bottom Left: Two-Way RM ANOVA. Factor: Stress, F (1, 4) = 0.3707, p=0.5755. Factor: Context, F (1, 4) = 0.1461. p=0.7218. Factor: Context x Stress, F (1, 4) = 0.6957. p=0.4512. Bottom Center: Two-Way RM ANOVA. Factor: Stress, F (1, 4) = 0.1235, p=0.7430. Factor: Context, F (1, 4) = 0.07882. p=0.7928. Factor: Context x Stress, F (1, 4) = 0.3309. p=0.5959. Bottom Right: Two-Way RM ANOVA. Factor: Stress, F (1, 4) = 0.7412, p=0.4378. Factor: Context, F (1, 4) = 0.008319. p=0.9317. Factor: Context x Stress, F (1, 4) = 0.09754. p=0.7704. **B** Visualization of MS neurons and MS to DH projections after injection of Cre-dependent AAV-GFP in Chat-Cre mice. **C** Top, localization of inhibitory DREADD and CNO infusions used for inhibition of MS to DH cholinergic projections by combining AAV-hM4Gi expression in MS to DH projections with injection of CNO in the DH. Cannulation was performed 72 hours before behavioral tests. Middle, experimental design depicting the timing of different circuit and behavioral manipulations. Bottom, reduced generalization of freezing in SD mice injected into DH with CNO. Bottom Left: Two-way RM ANOVA. Factor: Drug, F (1, 12) = 10.41, p=0.0073. Factor: Context, F (1, 12) = 20.03, p=0.0008. Factor: Drug x Context, F (1, 12) = 8.858, p=0.0116. n = 6 mice in Veh group, n = 8 mice in CNO group. Bottom Right: Mann Whitney Test. Sum of Ranks: 66 (Veh), 39 (CNO). p=0.0043.

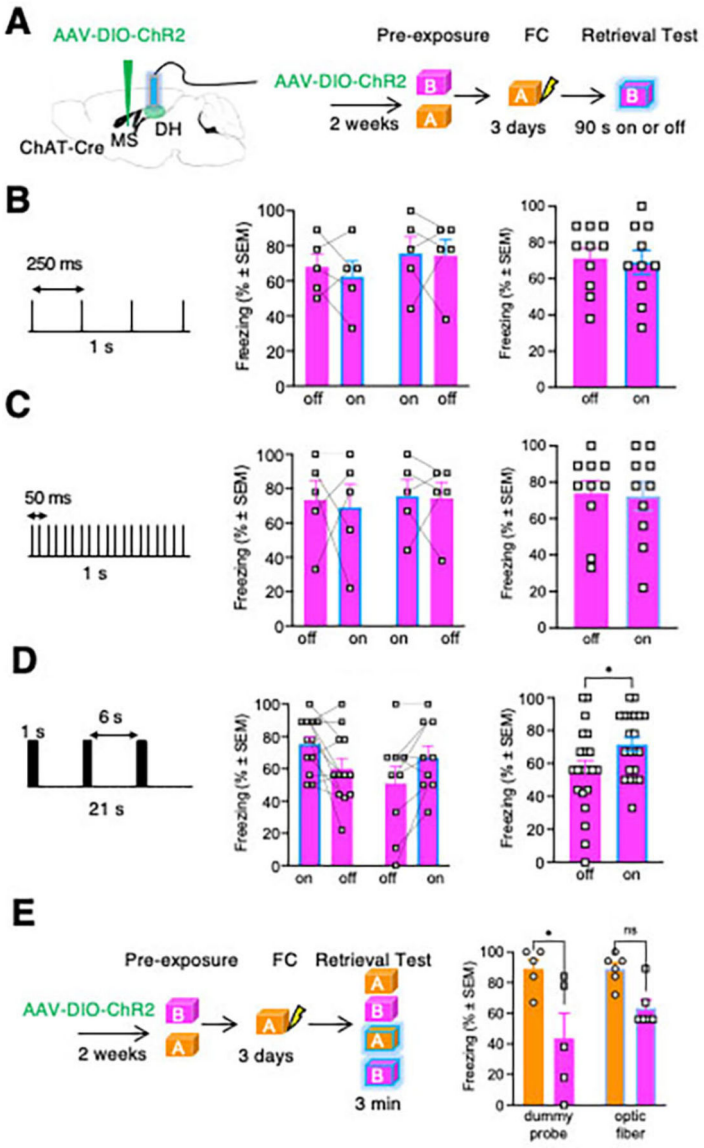

Fig 3: Optogenetic stimulation of MS-DH projections increases freezing in Context B.

A Timeline of opsin infusion in the MS and optogenetic stimulation of the DH. **B** Tonic 4 Hz optogenetic stimulation of DH did not affect freezing during the retrieval test in context B. The stimulation schedule is shown on the left, individual freezing responses during alternating on- or off-stimulation cycles are shown in the middle, and the combined data are on the right. Paired T-test, p=0.7445. n=10 mice. **C** Tonic 20 Hz optogenetic stimulation of DH did not affect freezing during the retrieval test in Context B. The stimulation schedule is shown on the left, individual freezing responses during alternating on- or off-stimulation cycles are shown in the middle, and the combined data are on the right. Paired T-test, p=0.8769. n=10 mice. **D** Burst 20 Hz optogenetic stimulation of DH significantly increased freezing in Context B in mice trained in Context A. The stimulation schedule is shown on the left, individual freezing responses during alternating on- or off-stimulation cycles are shown in the middle, and the combined data are on the right. Paired T-test, p=0.0022.

n=21 mice. **E** A similar effect of burst 20 Hz optogenetic stimulation of DH resulting in generalization of freezing is found using a between subject design. Two-way ANOVA. Factor: Device, $F(1, 18) = 1.244$, $P=0.2793$. Factor: Context, $F(1, 18) = 16.34$, $P=0.0008$. Factor: Device x Context, $F(1, 18) = 1.287$, $P=0.2714$. n = 5 mice in each dummy group (A group, B group), n = 6 mice in each device group (A group, B group).

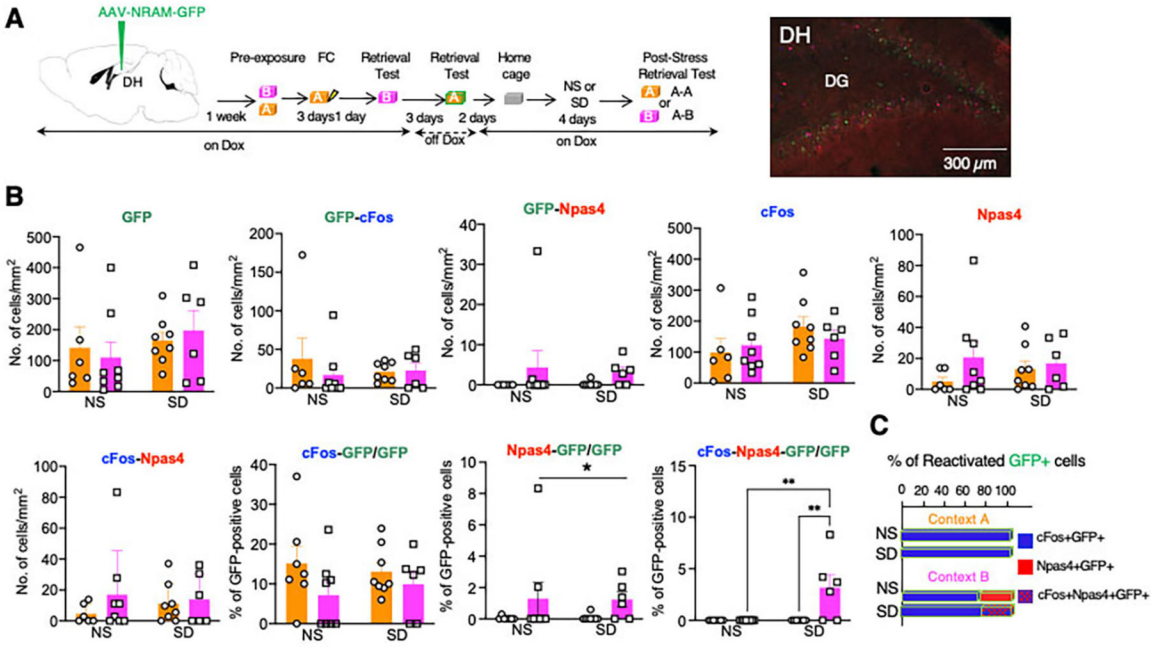

Fig 4: SD alters the reactivation of NRAM-GFP expressing neurons assessed by co-localization with cFos and Npas4

A Left, timeline of AAV9-*N*-RAM-d2tTA-TRE-GFP infusion, Dox regimen, and retrieval tests. As in the previous experiment, labeling of DH neurons with NRAM-GFP was performed at the first retrieval test in Context A, whereas reactivation was assessed after the second retrieval test either in Contexts A (A-A) or B (B-B). Middle, illustration of triple labeling of DG neurons with GFP, cFos, and Npas4. Right, illustration of GFP labeling in mice kept ON-Dox during the entire behavioral paradigm. **B** The number of GFP-, cFos-, and Npas4-positive DG neurons and their combinations after the post-stress retrieval test of SD mice or corresponding retrieval test of NS mice. The number of Npas4/GFP-co-labelled neurons was significantly increased after retrieval in Context B, whereas the number of triple labeled cFos/Npas4/GFP neurons was only detected in SD but not NS mice. *p < 0.05. Two-Way ANOVA. GFP: Stress F (1, 24) = 1.127, P=0.2990. Context F (1, 24) = 0.0001643, P=0.9899. Stress x Context F (1, 24) = 0.3764, P=0.5453. n = 6–8 mice in each group. GFP-cFos: Stress F (1, 24) = 0.1462, P=0.7056. Context F (1, 24) = 0.4782, P=0.4959. Stress x Context F (1, 24) = 0.6292, P=0.4354. n = 6–8 mice in each group. GFP-Npas4: Stress F (1, 24) = 0.0362, P=0.8506. Context F (1, 24) = 2.147, P=0.1558. Stress x Context F (1, 24) = 0.08050, P=0.7791. n = 6–8 mice in each group. cFos: Stress F (1, 24) = 2.324, P=0.1404. Context F (1, 24) = 0.05052, P=0.8241. Stress x Context F (1, 24) = 0.8190, P=0.3745. n = 6–8 mice in each group. Npas4: Stress F (1, 24) = 0.08408, P=0.7743. Context F (1, 24) = 1.762, P=0.1968. Stress x Context F (1, 24) = 0.6845, P=0.4162. n = 6–8 mice in each group. cFos-Npas4: Stress F (1, 24) = 0.05915, P=0.8099. Context F (1, 24) = 1.111, P=0.3024. Stress x Context F (1, 24) = 0.4367, P=0.5024. n = 6–8 mice in each group. cFos-GFP/GFP: Stress F (1, 25) = 0.01053, P=0.9191. Context F (1, 25) = 2.917, P=0.1000. Stress x Context F (1, 25) = 0.5415, P=0.4687. n = 6–8 mice in each group. Npas4-GFP/GFP: Stress F (1, 25) = 0.02197, P=0.8834. Context F (1, 25) = 4.470, P=0.0446. Stress x Context F (1, 25) = 0.04054, P=0.8421. n = 6–8 mice in each

group. cFos-Npas4-GFP/GFP: Stress F (1, 24) = 8.682, P=0.0070. Context F (1, 24) = 8.682, P=0.0070. Stress x Context F (1, 24) = 8.682, P=0.0070, n = 6–8 mice in each group. **C** In the A-A condition, all reactivated GFP neurons were positive for cFos, whereas in the A-B condition 18–20% of the reactivated neurons were Npas4-positive. Depending on the stress condition, the Npas4/GFP neurons were either a separate neuronal population (NS group) or a population co-labeled with cFos (SD).

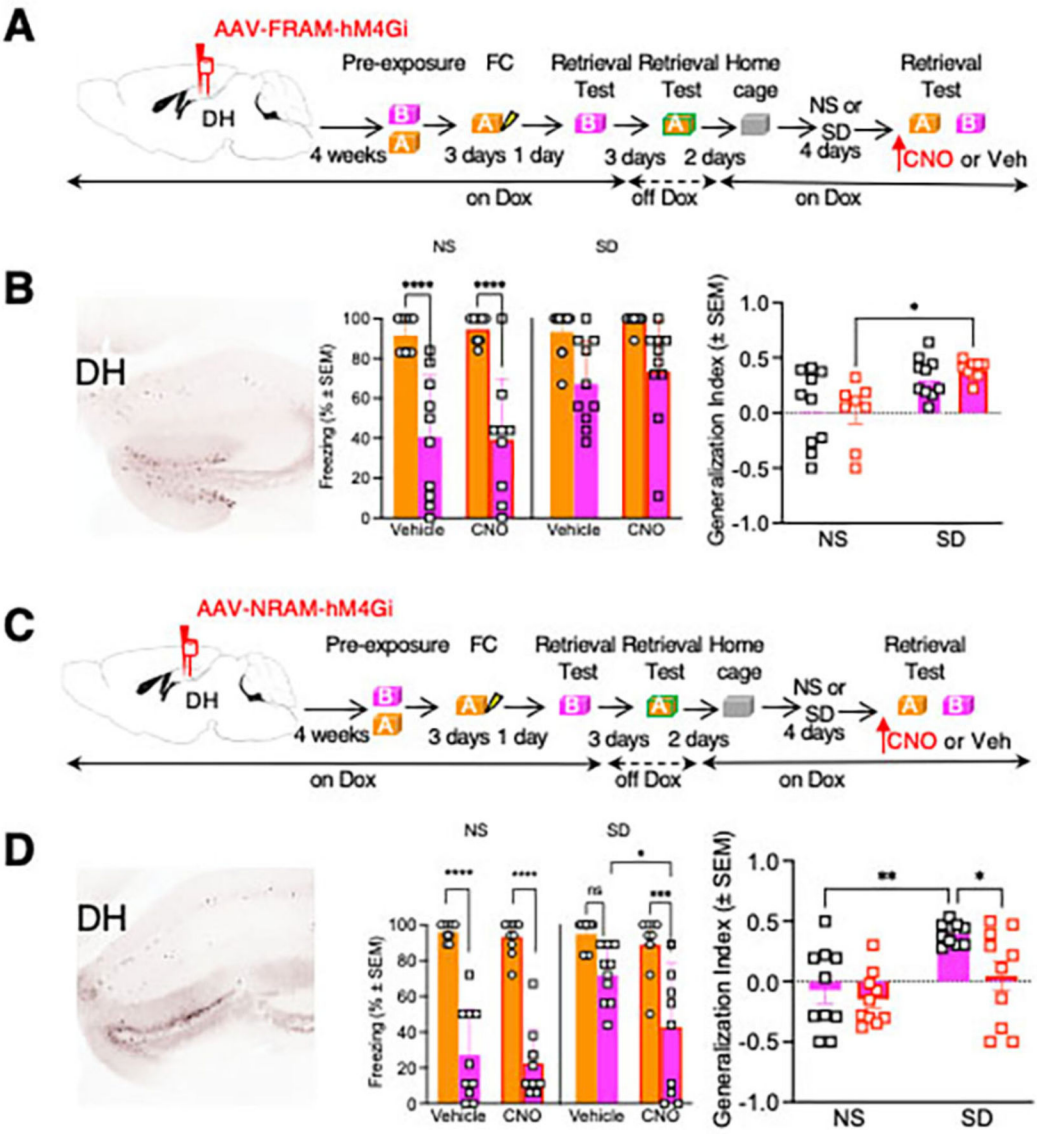

Fig 5: Chemogenetic inhibition of NRAM- but not FRAM-expressing neurons alleviates SIG

A Left, expression of FRAM-hM4Gi (AAV9-TRE-hM4Di-mCherry and AAV9-*F*-RAM-d2tTA-sEF1α-GFP) in DG. Right, timeline of the experimental manipulations. Cannulation was performed 72 hours before behavioral tests. **B** Left, freezing before or after SD in mice injected with Veh or CNO. SD significantly increased generalization. CNO did not affect freezing during the pre- or post-stress test. Right, similar effects were found with analysis of the generalization index. Left: Three-Way RM ANOVA. Factor: Drug, F (1, 17) = 0.7190, P=0.4083. Factor: Stress, F (1, 17) = 10.09, P=0.0055. Factor: Context, F (1, 17) = 55.95. P<0.0001. Factor: Context x Stress, F (1, 17) = 7.235. P=0.0155. Factor: Drug x Stress, F (1, 17) = 0.5723, P=0.4597. Factor: Drug x Context, F (1, 17) = 0.002591, P=0.9600. Factor: Stress x Context, F (1, 17) = 7.235, P=0.0155. Factor: Drug x Stress x Context, F (1, 17) = 0.0003833, P=0.9846. n=9–10 mice per group. Right: Two-Way RM ANOVA. Factor: Stress, F (1,17) = 9.367, p=0.0071. Factor: Drug, F (1,17) = 0.0005083, p=0.9251. Factor:

Stress x Drug, F (1,17) = 0.01760, p=0.8960. n=10 mice per group. **C** Left, expression of NRAM-hM4Gi (AAV9-TRE-hM4Di-mCherry and either AAV9-*N*-RAM-d2tTA-sEF1α-GFP) in DG. Right, timeline of the experimental manipulations. Cannulation was performed 72 hours before behavioral tests. **D** Left, freezing before or after SD in mice injected with Veh or CNO. SD significantly increased generalization, an effect significantly reduced by CNO. Right, SD significantly increased the generalization index, whereas CNO significantly attenuated this effect. Left: Three-Way RM ANOVA. Factor: Drug, F (1, 18) = 6.278, P=0.0221. Factor: Stress, F (1, 18) = 8.571, P=0.0090. Factor: Context, F (1, 18) = 149.7. P<0.0001. Factor: Context x Stress, F (1, 18) = 17.14. P=0.0006. Factor: Drug x Stress, F (1, 18) = 2.660, P=0.1203. Factor: Drug x Context, F (1, 18) = 2.833, P=0.1096. Factor: Stress x Context, F (1, 18) = 17.14, P=0.0006. Factor: Drug x Stress x Context, F (1, 18) =1.993, P=0.1751. n=10 mice per group. Right: Two-Way RM ANOVA. Factor: Stress, F (1,18) = 8.912, p=0.0079. Factor: Drug, F (1,18) = 5.823, p=0.0267. Factor: Stress x Drug, F (1,18) = 2.135, p=0.1612. n=10 mice per group.

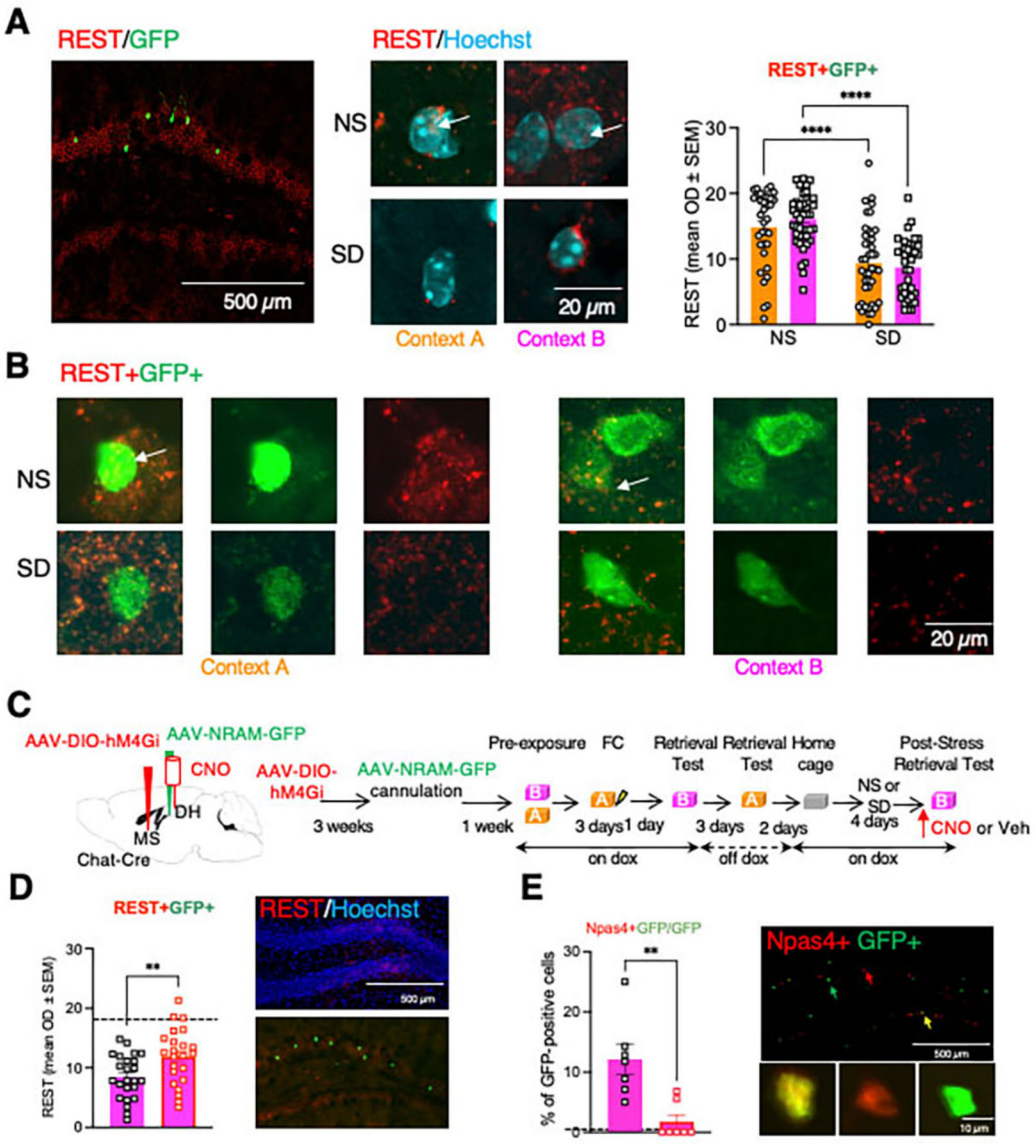

Fig 6: SD-induced reduction of REST levels in NRAM-GFP neurons was reversed by chemogenetic inhibition of MS-DH cholinergic projections

A Left, illustration of co-labelling of REST (red) and NRAM-GFP (green) in the DG. Middle, illustration of nuclear localization of REST in NS mice, and its reduction in SD mice. Right, analysis was performed and quantified for REST/GFP-positive neurons, showing a significant reduction of nuclear REST signals in this population. Two-Way ANOVA. Factor: Stress, $F(1, 155) = 64.12$, $p<0.0001$. Factor: Context, $F(1, 155) = 0.1531$, $p=0.6961$. Factor: Stress x Context, $F(1, 155) = 1.381$, $p=0.2418$. n= 35–43 per group. **B** Illustration of REST/NRAM-GFP co-labeling in NS and SD mice after exposure to Contexts A or B. **C** Left, localization of AAV-DIO hM4Gi infusion into MS, NRAM-GFP into DH, and cannula implantation in the DH. Right, timeline of the infusions, implantation, Dox regimen, and behavioral manipulations. **D** Left, injection of CNO partially but significantly restored REST levels. Dashed line corresponds to the mean density of REST signal in the NS group. Student's T Test, $t=2.742$, $df=45$, $p=0.0087$, n=23–24 per group. Right, REST

immunolabeling in the DG of SD mice counterstained with Hoechst (top) or co-labeled with NRAM-GFP (bottom). **E** Left, in NRAM-GFP labeled neurons, CNO decreased the levels of Npas4 levels. Dashed line corresponds to the number of Npas4/GFP-positive cells after exposure to context A. Student's T Test, t=3.798, df=12, p=0.0025, n=7 mice in each group. Right, illustration of immunolabeling of the DG (top) and individual neuronal populations (bottom).